Synthesis and Processing of PMR-15/LaRC-TPI Semi-IPN Systems

H. J. TAI,[1,*] B. Z. JANG,[1,†] and J. B. WANG[2,‡]

[1]Composites Research Labs, 201 Ross Hall, Auburn University, Alabama 36849, and [2]Yuen Foong Yu Paper Mfg. Co., Research Center, KaoHsiung, Taiwan, Republic of China

SYNOPSIS

To improve the fracture toughness of PMR-15 polyimide and to alleviate its high susceptibility to microcracking induced by thermal cycling, a thermoplastic polyimide, LARC-TPI, was incorporated to form a sequential semi-interpenetrating polymer network (semi-2-IPN). The imidization kinetics of LARC-TPI in the semi-IPNs were studied using a thermal gravimetric analyzer. Both the solvent and the glass transition temperature of the semi-IPN were found to have significant effects on the imidization kinetics. The kinetics could be modeled by a two-step reaction: the first step being a second-order reaction followed by a second step, which is a first-order diffusion-controlled reaction. Differential scanning calorimetry was chosen to investigate the curing of PMR-15 and PMR-15/LARC-TPI semi-IPNs. The curing process was well correlated by a first-order reaction kinetics, which suggested that the reverse Diels–Alder reaction of the Norbornene end group was the rate controlling step. The glass transition temperatures of these semi-IPNs were again found to play important an important role in dictating the curing kinetics. A higher proportion of LARC-TPI or a higher glass transition temperature of the semi-IPN prepolymer tended to result in a slower curing reaction. The optimum molding cycle of PMR-15 and PMR-15/LARC-TPI semi-IPNs were then determined from the obtained kinetics. © 1995 John Wiley & Sons, Inc.

INTRODUCTION

The approach of incorporating a tough thermoplastic resin into a brittle thermoset matrix resin has proven to be effective in improving the fracture toughness of the thermoset. A recent trend for synthesizing synergistic matrix resins for high-performance composite applications has involved semi-interpenetrating polymer network (semi-IPN) methods. The semi-IPN methods have the advantages of great versatility in formulation and the low cost of material development. These methods are capable of providing a spectrum of material properties that can be tailored to fulfill different requirements that cannot be achieved by individual polymer components.

PMR-15 polyimide is the leading baseline polyimide matrix resin in structural composites for high-temperature applications.[1] PMR-15 and bismaleimide (BMI) matrix composites have been considered for use as structural elements in the future high-speed commercial transport aircraft (HSCT).[2] PMR-15 possesses excellent thermo-oxidative properties that can withstand temperatures above 300°C for prolonged periods.[2] However, this resin is very brittle and suffers from severe microcracking problems under thermal cycling, which could lead to a significant reduction in the compressive strength.[3] Another drawback of this material has been the difficulty in reproducibly processing thick section laminates due to its complex chemistry.[4]

PMR-15 is an addition-type polyimide developed by NASA in the early 1970s. The complex synthetic chemistry of PMR-15 is still an important subject in recent research efforts.[1,5,6] The ideal synthesis procedure is shown in Figure 1. In the first step,

* Now with Plastics Industry Development Center, Taichung, Taiwan.

† To whom correspondence should be addressed.

‡ Now with Department of Chemical Engineering, KaoHsiung Polytechnic Institute, KaoHsiung, Taiwan.

Journal of Applied Polymer Science, Vol. 58, 2293–2306 (1995)
 CCC 0021-8995/95/122293-14

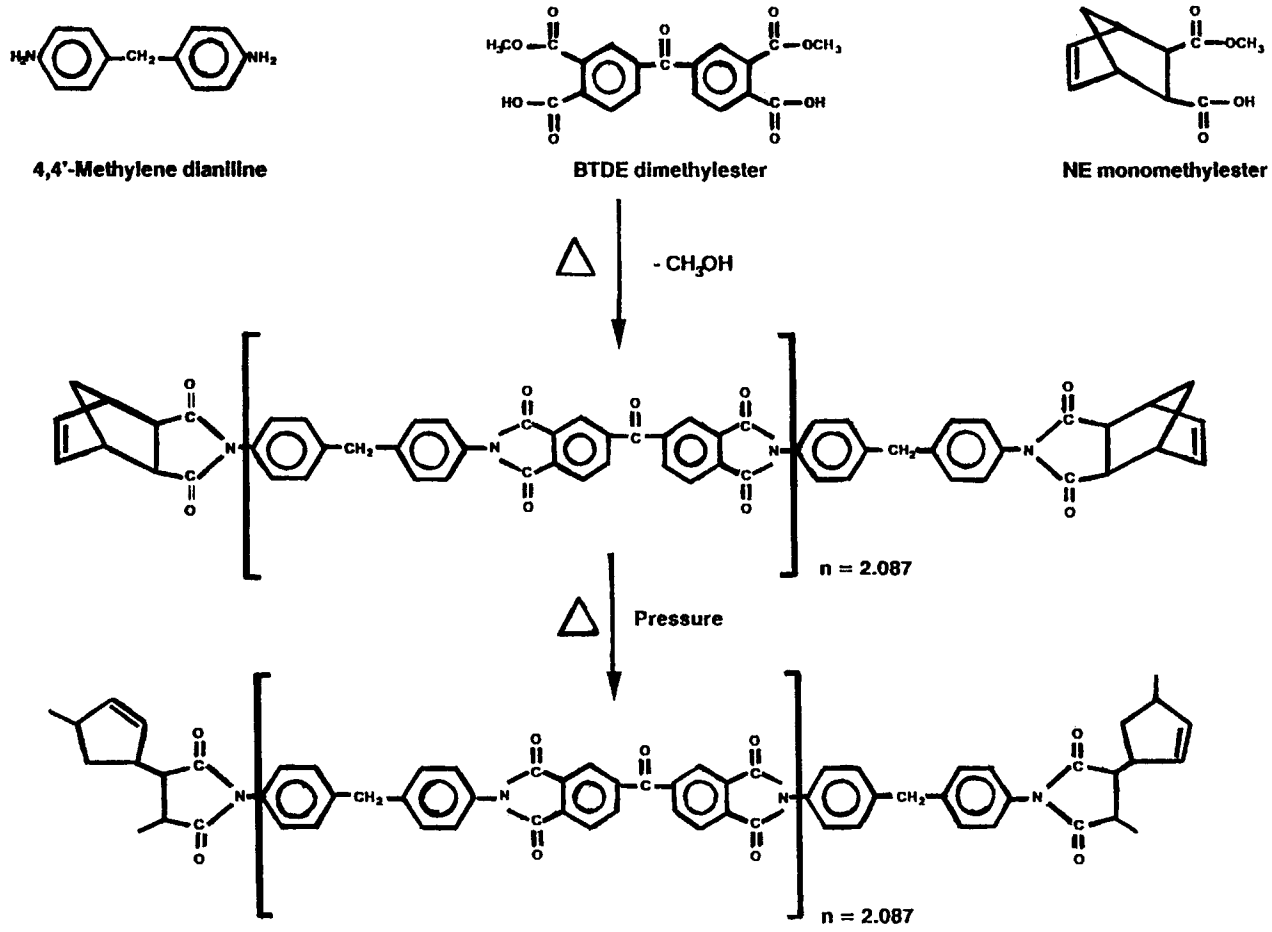

Figure 1 Schematic of PMR-15 synthesis route.

three monomers, nadiac ester (NE), semi-ester of 3,3',4,4'-benzophenone tetra-carboxylic acid (BTDE), and 4,4'-diaminodiphenylmethane (MDA) are mixed at a suitable stoichiometric ratio in methanol. They react to form poly(amic acid) at room temperature. Following imidization at around 150°C, the polyimide oligomer is obtained. The resulting prepolymer before crosslinking will have a number-average molecular weight of approximately 1500 g/mol if a molar ratio of NE : BTDE : MDA = 2 : 2.087 : 3.087 is used.[7]

It is well accepted that PMR-15 crosslinks via reverse Diels–Alder (RDA) chemistry.[3,8] A combined TGA/DTA/MS analysis[3] showed that cyclopentadiene evolved at 200°C and to a greater extent at 260°C, which indicated that RDA is the operative reaction mechanism. Above 290°C all the molecules are essentially tied into the crosslinked network. However, the detail of crosslinking reactions including chain initiation, propagation, and termination remains unclear and is still a subject of active research. Because a direct investigation on PMR-15 would be too involved, most of the research efforts on reaction mechanisms were conducted with simpler model compounds.[5,7]

Thermoplastic polymers have long been recognized to provide higher toughness, damage tolerance, and delamination resistance as compared to their thermoset counterparts.[9] LARC-TPI is a linear thermoplastic polyimide developed by NASA in the late 1970s as a high-temperature adhesive for aerospace applications.[10] It is now used in the forms of varnish, powder, film, and prepreg. LARC-TPI offers excellent thermal stabilities and good mechanical properties, but is relatively difficult to process.

Like most thermoplastic polyimides, the synthesis of LARC-TPI thermoplastic polyimide follows a two-step polycondensation method, as shown in Figure 2. The first step is the formation of poly(amic acid) by a second-order acylation reaction of diaminobenzophenone (DABP) with benzophenone tetracarboxylic dianhydride (BTDA) in diglyme.[6] The second step is the thermal dehydrocyclization of the poly(amic acid) at around 200°C. In this step, a variety of side reactions are involved. Several byproducts such as anhydride, isoimides, and noncyclic

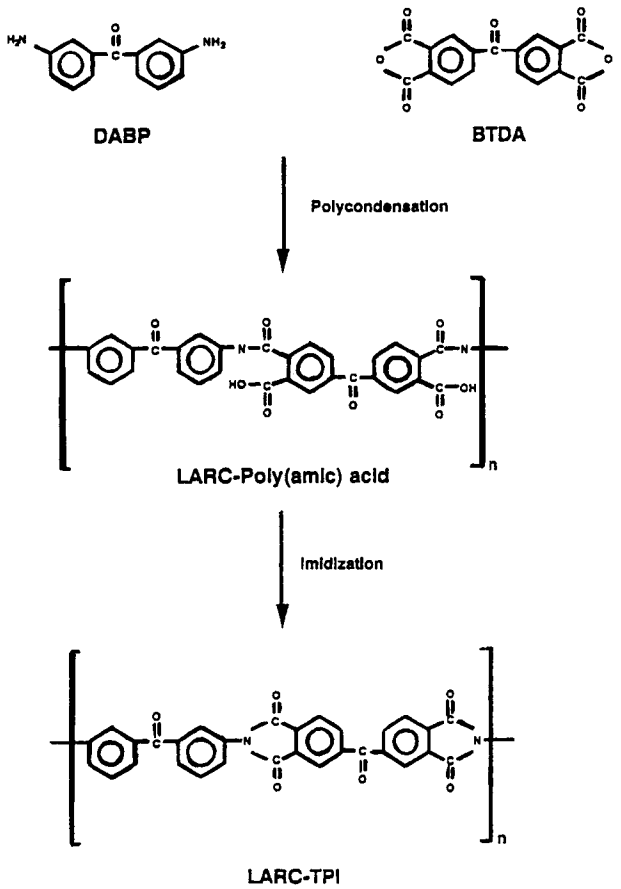

Figure 2 Schematic of LARC-TPI synthesis route.

imides may form at this stage.[11] The presence of solvent markedly influences imidization by forming complexes with the poly(amic acid) precursor.[1,12]

PMR-15 is a very brittle material with a G_{Ic} (fracture energy) value of approximately 90 J/m^2,[13] while LARC-TPI is a relatively tough thermoplastic with a G_{Ic} value of up to 1800 J/m^2.[13] PMR-15 matrix-based composites, therefore, exhibit very poor damage tolerance. These composites are also highly vulnerable to microcracking induced by thermal cycling, which could lead to a 50% reduction in the compressive strength after only 1500 cycles.[3] Many approaches have been employed to toughen the PMR-15 matrix, including the synthesis of semi-IPN by incorporating a tough thermoplastic into the thermosetting matrix.[13,14] The methodology involves combining easy-to-process but brittle thermosetting polyimides with tough but difficult-to-process thermoplastic polyimides without compromising the best properties of each constituent.

The PMR-15/LARC-TPI semi-IPN polyimide is a promising candidate matrix for high-temperature composites. However, LARC-TPI polymerizes by imidization with the evolution of water molecules, which could lead to possible formation of voids during processing. Hence, a primary goal of the present study was to gain a clear understanding of the imidization kinetics of LARC-TPI and the crosslinking kinetics of PMR-15, which was essential to the successful synthesis and processing of these PMR-15/LARC-TPI semi-IPNs. Studies of PMR-15 reactions by means of differential scanning calorimetry (DSC) and thermal gravimetric analysis (TGA) have been quite difficult because the amount of heat evolved is low and several impurities and side reactions are involved.[3,11] However, both techniques are still considered to be the most effective ones for studying the reaction kinetics of thermoset resins.[1] Therefore, these thermal analysis techniques, in conjunction with FT-IR, were used to investigate the PMR-15/LARC-TPI semi-IPN systems.

EXPERIMENTAL

Materials

The materials used in this study included PMR-15 prepolymer molding powder supplied by Dexter Corporation and LARC-TPI in the form of the precursor poly(amic acid) powder supplied by Mitsui Toatsu Chemicals Inc. All these materials were stored in a desiccator at room temperature to avoid absorption of moisture.

Preparation of Semi-IPNs

The semi-IPN powders were prepared in the following steps: the as-received molding powders of PMR-15 prepolymer and LARC-poly(amic acid) were first dried under a vacuum (less than 0.1 Torr) at 100°C for 1 h to eliminate any absorbed moisture. Spectra grade dimethyl acetamide (DMAc) was used as the solvent. The powder-to-solvent weight ratio was 20 : 80 for each composition of semi-IPNs. Small quantities of the dried powders of PMR-15 and LARC-poly(amic acid) precursor were poured alternately into the stirring DMAc. Stirring of the solution was maintained for 2 h to completely dissolve all solid particles in the DMAc. This stirring also ensured that the mixing of the two components in the solution was complete. The solution at this point appeared dark brown.

The homogeneous solution was poured into deionized distilled water under stirring, which served as a nonsolvent. A light yellow precipitate was collected by filtering the colloid and was washed with deionized distilled water three times to minimize residual DMAc in the samples. The precipitate was

dried under vacuum (less than 0.1 Torr) for 2–3 days at room temperature and then further dried at 100°C under vacuum for 2 h. After drying, the material was kept in a desiccator until ready for use.

Thermal Analysis

A Perkin–Elmer TGA-7 (Thermo-Gravimetric Analyzer) was used to monitor the weight losses of LARC-TPI, PMR-15, and their semi-IPNs at a ramp rate of 10°C/min from 50 to 600°C. TGA was also utilized to measure the imidization kinetics of LARC-TPI at various ramp rates ranging from 5 to 20°C/min over the temperature range of 50 to 300°C. The sample weights were between 5 to 20 mg.

A Perkin–Elmer DSC-7 (Differential Scanning Calorimeter) was used to monitor the crosslinking kinetics of PMR-15 and PMR-15/LARC-TPI semi-IPNs and to measure their glass transition temperatures. The sample weights were between 10 to 15 mg. For measurements of crosslinking kinetics, the samples were kept in the Perkin–Elmer TGA-7 at 100 and 200°C for 30 min before each DSC run. For measuring the glass transition temperatures, samples were staged in the TGA at 100, 200, 250, 300, and 350°C each for 30 min to ensure that the imidization and crosslinking reaction had been completed.

FTIR Spectroscopy

Both diffuse reflectance and transmission infrared spectroscopy were conducted by using a Matteson Polaris FTIR (Fourier Transform Infrared). Transmission spectroscopy data were obtained using the KBr pellet method. The pellet was made by pressing a 1% by weight powder sample mixed with IR grade KBr powder. For monitoring the reaction *in situ*, a Spectra-Tech Collector diffuse reflectance accessory equipped with a controlled environmental chamber was employed to measure the diffuse reflectance spectra by FTIR. The samples were in powder form. All spectra were collected over the wavenumber range of 2000 to 400 cm^{-1}. For the kinetics study, the spectra averaged over 64 scans were taken at a resolution of 4 cm^{-1}.

RESULTS AND DISCUSSION

To make a semi-IPN, both component materials must be soluble in common solvents, e.g., NMP, DMF, and DMAc. Because LARC-TPI is essentially insoluble in those solvents, its precursor poly(amic acid) was used in the synthesis of the PMR-15/LARC-TPI semi-IPN. The thermal imidization kinetics were, thus, important for the processing of this semi-IPN. Because there was a weight loss due to the release of water molecules during the course of imidization, TGA was chosen to follow the reaction.

Most researchers use isothermal conditions to study the reaction kinetics. However, the temperature range within which the reaction-induced property change can be detected within the capability limit of the instrument is quite narrow. Thus, the isothermal method could lead to a larger error in estimating kinetic parameters, namely, the activation energy and preexponential frequency factor. By assuming no change in reaction mechanism during thermal imidization of the LARC-poly(amic acid) resin, an alternative dynamic scan method was employed instead.

Before each TGA temperature scan, LARC-poly(amic acid) was kept at 100°C for 30 min to remove any absorbed moisture. Three scan rates of 5, 10, and 20°C/min were used to scan dynamically from 100 to 360°C. The results are shown in Figure 3. The higher the ramp rate, the higher the temperature for the imidization to be complete. The imidization takes place between 180 and 300°C. Assuming that the reaction kinetics is of the simple nth order reaction and that the reaction constant can be expressed by an Arrhenius equation, then

$$\frac{dx}{dt} = k(1-x)^n = A\exp\left(-\frac{E_a}{RT}\right)(1-x)^n \quad (1)$$

where k is the reaction constant, x is the degree of conversion obtained by the amount of weight loss divided by total weight loss, n is the reaction order, A is the preexponential frequency factor, and E_a is

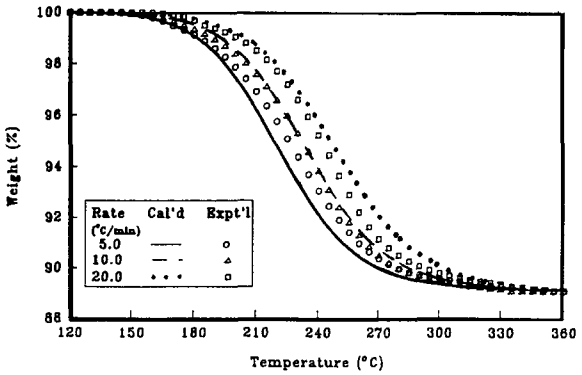

Figure 3 The weight losses of imidizing LARC-poly(amic acid) under dynamic TGA scans. The theoretical curves were calculated by using nth order kinetics.

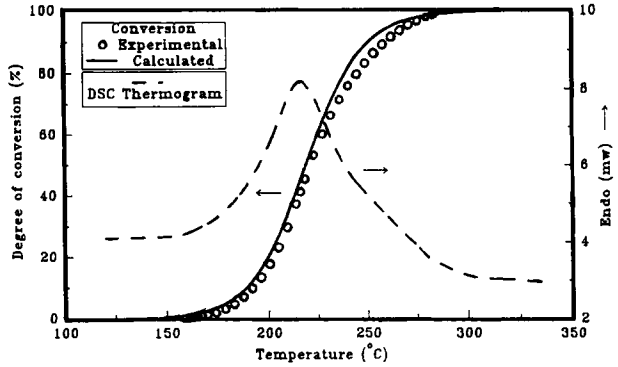

Figure 4 A DSC thermogram and the degree of conversion of LARC-TPI at a ramp rate of 10°C/min.

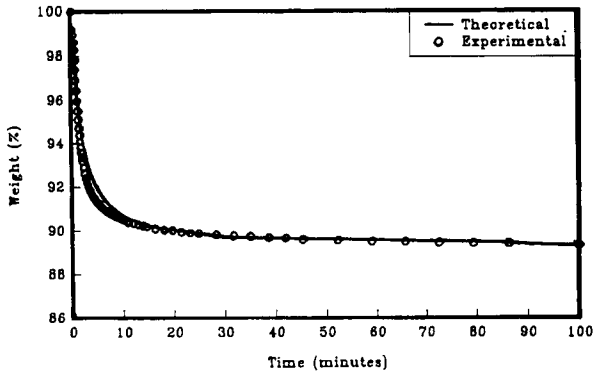

Figure 5 The weight losses of imidizing LARC-poly(amic acid) at 250°C. The theoretical curve was calculated by using simple *n*th order kinetics.

the activation energy. By taking the logarithm on both sides, then

$$\ln \frac{dx}{dt} = \ln A - \frac{E_a}{RT} + n \ln (1 - x) \qquad (2)$$

The kinetic parameters were estimated by using a multiple variable regression method with $\ln(dx/dt)$ as the dependent variable, and $1/T$ and $\ln(1-x)$ as the independent variables. The parameters of eq. (2) were determined to be: $n = 1.88$, $A = 5.35 \times 10^9$ min^{-1}, and $E_a = 98.1$ kJ/mol. Theoretical curves also are shown in Figure 3. The calculated values fit the experimental curve with a ramp rate of 10°C/min very well, but somewhat underestimate the 5°C/min curve and overestimate the 20°C/min curve.

A similar method was applied to analyze the results obtained with DSC, which was conducted at a ramp rate of 10°C/min, as shown in Figure 4. The parameters obtained were: $n = 1.85$, $A = 6.91 \times 10^9$ min^{-1}, and $E_a = 128$ kJ/mol. The endothermic heat of imidization was 200 J/g. Both TGA and DSC results seemed to suggest that the imidization of LARC-poly(amic acid) was an apparent second order reaction (with n near 2). Because imidization involves only intramolecular reactions, a second-order reaction implies that the residual solvent played a major role in the imidization of LARC-TPI. The interplay between solvents and the thermal cyclization of LARC-TPI has been recognized, and the kinetics has been studied with FTIR in an earlier investigation.[15] Amide solvents form strongly hydrogen-bonded complexes with the carboxyl group and will enhance the imidization by allowing the reaction species to attain favorable conformations for cyclization.[15,16]

In earlier reports,[15-17] it was proposed that the imidization proceeded by two mechanisms under isothermal conditions. At first, an initial fast cyclization took place, which was followed by a slower cyclization process. The simple *n*th order kinetic parameters obtained by the TGA experiment were used to estimate the reaction under isothermal conditions. As shown in Figure 5, when LARC-poly(amic acid) was imidized at 250°C isothermally, the predicted curve agreed closely with the experimental results. No fast–slow cyclization phenomenon was observed.

However, a large discrepancy existed between the experimental and the calculated curves when the imidization was carried out at 220°C for 1 h and then 250°C for another hour, as shown in Figure 6. Because the glass transition temperature for LARC-TPI is about 250°C, there seems to be a distinct reaction mechanism for reactions below 250°C. Because the imidization mechanisms are complex, several explanations have been offered for the phenomena of fast and slow cyclization processes. They are: different reactivity of the *o*-carboxycarboxamide,[16] loss of the residual solvent that enhances the

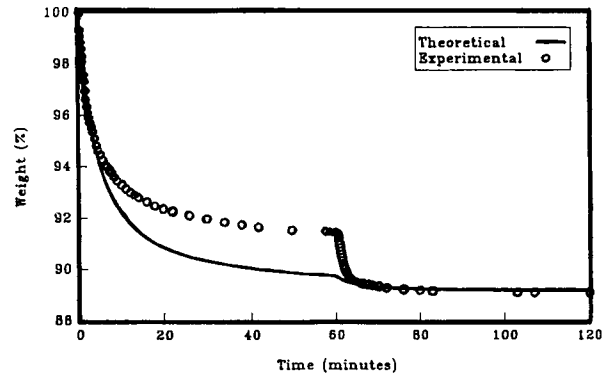

Figure 6 The weight losses of imidizing LARC-poly(amic acid) at 220°C and 250°C each for 1 h. The theoretical curve was calculated by simple *n*th order kinetics.

process,[17] or the decrease of molecular mobility due to the increase of the glass transition temperature.[16]

Assuming the increase in the glass transition temperature was the reason for the slowing down of the reaction, a reaction in a series model was proposed to take into account the slowing down of the reaction under isothermal condition

$$A \xrightarrow{k_1} B \xrightarrow{k_2} C \tag{3}$$

The first step was the formation of a favorable conformation for cyclization with the interaction of solvent molecules. This was a second-order reaction. The second step was the formation of imide rings, which involved the diffusion of water and solvent molecules. This step was assumed to be a first-order reaction. Neglecting the change in density, the rate of reaction could be written as

$$\frac{dy_1}{dt} = -k_1 y_1^2 \tag{4a}$$

$$\frac{dy_2}{dt} = k_1 y_1^2 - k_2 y_2 \tag{4b}$$

$$\frac{dx}{dt} = k_2 y_2 \tag{4c}$$

where y_1, y_2 are the weight fractions of the LARC-TPI and the intermediate, respectively; x is the degree of conversion and can be solved by using eq. (4c). The initial conditions are $y_1 = 1$ and $y_2 = x = 0$. The solutions to these differential equations with k_1, k_2 being constant are[18]

$$y_1 = \frac{1}{(1 + k_1 t)}$$

$$y_2 = r\, e^{-r/y_1}\left[\frac{1}{r} e^{r} - y_1 e^{r/y_1} - Ein(r) + Ein\left(\frac{r}{y_1}\right)\right]$$

$$x = 1 - y_1 - y_2 \tag{5}$$

where

$$Ein(x) = \int_{-\infty}^{x} \frac{e^x}{x}\, dx \tag{6}$$

and $r = k_2/k_1$.

In a dynamic scan or when the reaction temperature is above the glass transition temperature, $k_2 >> k_1$. The first step controlled the reaction rate and the reaction followed an apparent second-order rate law. When the isothermal reaction temperature was far below the glass transition temperature or when the degree of conversion was high, $k_1 >> k_2$, the second step controlled the rate of reaction. The reaction was diffusion controlled and the activation energy was assumed to be

$$E_a = E_{a_0} + \alpha\,(T_g - T) \tag{7}$$

Then the rate of reaction was of the following form:

$$\frac{dx}{dt} = k_2\,(1 - x)$$

$$= A' \exp\left(-\frac{\alpha(T_g - T)}{RT}\right)(1 - x) \tag{8}$$

To estimate the parameters in eq. (4), the above dynamic TGA scan data were used, assuming $k_2 >> k_1$. A plot of $\ln[(dx/dt)/(1-x)^2]$ vs. $1/T$ is shown in Figure 7. With the application of linear regression, the kinetics parameters obtained were: frequency factor $A = 3.64 \times 10^{11}\ \text{min}^{-1}$, and activation energy $E_a = 114$ KJ/mol. The experimental values do not fit into a straight line because the exact reaction order obtained from the multiple variable regression method was 1.88, not 2.

To measure the diffusion controlled step, a series of isothermal TGA scans were performed. The LARC-poly(amic acid) resin samples were staged at three isothermal temperatures, 208, 218, and 228°C for 24 h. Because the second step was assumed to be a first-order reaction, the conversion was independent of the initial concentration. Only the final portions of weight loss in the thermogram were utilized in the linear regression to estimate k_2, by assuming the second step now being the dominating mechanism. A plot of $\ln[(dx/dt)/(1-x)]$ vs. $(T-T_g)/T$ is shown in Figure 8. The kinetic constants obtained by applying linear regression were: $A' = 7.632 \times 10^{-3}\ \text{min}^{-1}$, $\alpha = 247.4$ J/°K mol. The

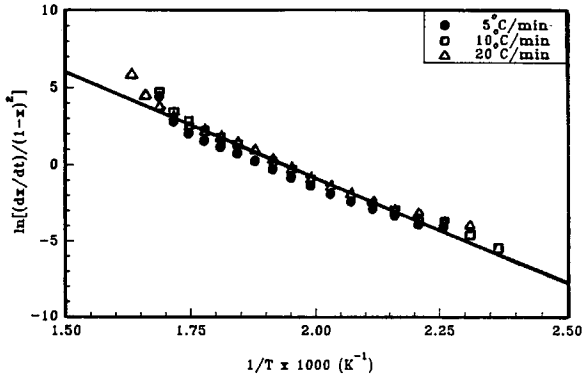

Figure 7 Linear regression on the TGA dynamic scan data of LARC-TPI assuming a second-order reaction in the first step.

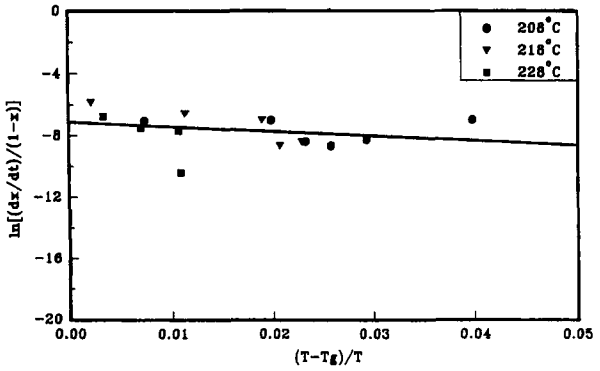

Figure 8 Linear regression on the TGA dynamic scan data of LARC-TPI assuming a first-order reaction in the second step.

experimental data points scatter more in this figure because the use of only a small portion of the weight loss data from the TGA experiments was utilized.

The analytical solutions of eq. (4) under isothermal conditions were not applicable in the study because the kinetic constant k_2 of the diffusion control step was not a constant. As seen in eq. (8), k_2 was a function of T_g, which in turn, was a function of the degree of conversion. There are several correlation equations for the glass transition temperature as a function of conversion for thermosetting polymers.[19] In this study, for simplicity, the simplest rule-of-mixtures relationship was chosen, where T_g was expressed as

$$T_g = T_{g_{\text{LaRC-poly(amic acid)}}}(1 - X) + T_{g_{\text{LaRC-TPI}}}X \quad (9)$$

where the glass transition temperatures of both LARC-poly(amic acid) and LARC-TPI could be measured experimentally and will be discussed in detail in a later section.

The Richardson extrapolation and the Bulirsch–Stoer method[20] were used to solve the differential equation set (4) numerically with the same initial conditions, T_g being expressed in eq. (9) and k_2 in eq. (8). The experimental and theoretical results predicted by both the simple second-order reaction and the modified two-step reaction are shown in Figure 9. The simple second-order mechanism predicted a much faster completion time, while the two-step mechanism agreed reasonably well with the experimental results. This analysis was consistent with the conclusion[16] that the decrease in molecular mobility due to an increase in the glass transition temperature accounted for the fast and slow cyclization phenomena.

The time needed for 95% completion of imidization could be calculated and is shown in Figure

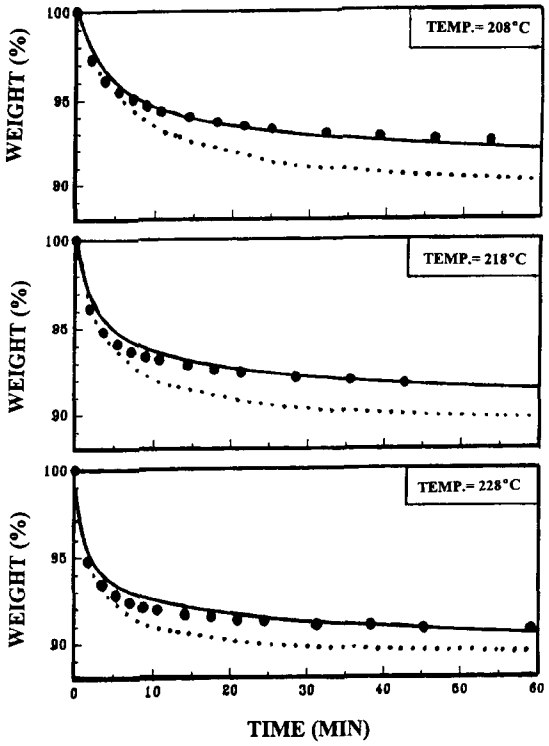

Figure 9 The weight losses of LARC-TPI at different isothermal temperatures. Keys: (——) Two-step kinetics; (----) simple *n*th order kinetics; (●) experimental values.

10. This provided an estimation of the processing time to complete the imidization process in the synthesis. In addition, along with the use of the kinetic parameters of PMR-15, the time needed at each temperature in the study of the kinetics of semi-IPNs could be estimated. The material was staged at a temperature where imidization could be completed without any significant degree of cure of the PMR-15. The curing kinetics of these semi-IPNs

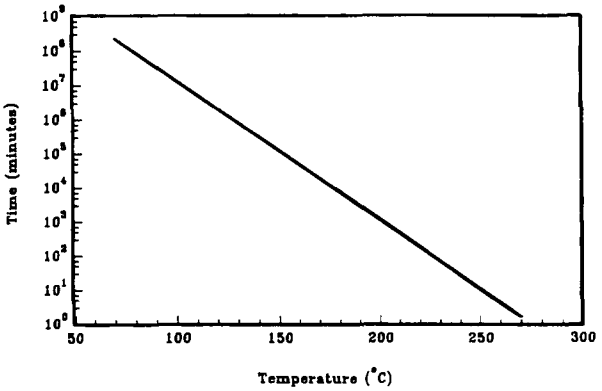

Figure 10 The time needed for a 95% completion of isothermal imidization of LARC-TPI predicted by two-step kinetics.

could then be studied without the interference of imidization of LARC-TPI. The parameters obtained are listed in Table I.

DSC was employed to study the curing kinetics of imidized PMR-15 prepolymers. Because PMR-15 cures via addition polymerization without any weight loss, TGA was not an appropriate tool. The enthalpy change involved in the curing of PMR-15 resin is relatively small, so monitoring the thermal polymerization at a constant temperature is difficult. Besides, isothermal scans also have the aforementioned drawbacks. Thus, DSC dynamic scans were chosen to reveal the curing kinetics and to estimate the reaction parameters.

Temperature increment rates of 5, 10, 15, and 20°C/min were used to follow the kinetics. A representative DSC thermogram at a ramping rate of 10°C/min is shown in Figure 11. The reaction was endothermic with a heat of reaction $\Delta H = 45 \pm 10$ J/g. The onset of the reaction was about 250°C and the reaction was completed at about 315°C. A simple nth order reaction [eq. (1)] was also assumed to follow the curing kinetics. Using the multiple variables regression method, the following parameters were obtained: the activation energy E_a = 141 kJ/mol, the preexponential frequency factor $A = 6.6 \times 10^{12}$ min^{-1}, and the reaction order n = 0.95. The kinetic parameters are listed in Table I. The reaction followed apparent first order kinetics (n close to 1). The rate determining step in the reaction was deduced to be the single molecule dissociation involved in the reverse Diel–Alder reaction. This step was

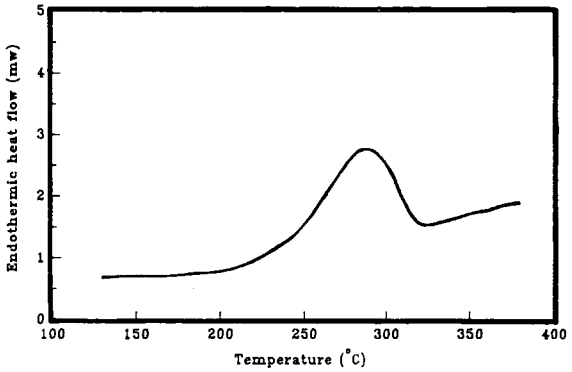

Figure 11 A typical DSC thermogram of PMR-15 scanned at a ramp rate of 10°C/min.

Table I Kinetic Constants of LaRC-TPI, PMR-15 and Their Semi-IPNs

	From TGA Data	From DSC Data
	LaRC-TPI	
One-step mechanism	$A = 3.21 \times 10^{11}$ min^{-1} Ea = 98.1 kJ/mol n = 1.88 $\Delta H = 150 \pm 10$ J/g	$A = 4.15 \times 10^{11}$ min^{-1} Ea = 128 kJ/mol n = 1.85
Two-step mechanism	$A_1 = 3.64 \times 10^{11}$ min^{-1} Ea = 114 kJ/mol n = 2	$A_2 = 7.63 \times 10^{-3}$ min^{-1} α = 247.4 J/°K mol n = 1
	PRM-15	
	$A = 6.6 \times 10^{12}$ min^{-1} Ea = 141 kJ/mol n = 0.95 $\Delta H = 45 \pm 10$ J/g	$A = 9.24 \times 10^{12}$ min^{-1} Ea = 142 Kj/mol n = 1
	PMR-15 85%/LaRC-TPI 15%	
	$A = 4.98 \times 10^{15}$ min^{-1} Ea = 174 KJ/mol n = 1	
	PMR-15 75%/LaRC-TPI 25%	
	$A = 6.82 \times 10^{17}$ min^{-1} Ea = 199 KJ/mol n = 1	

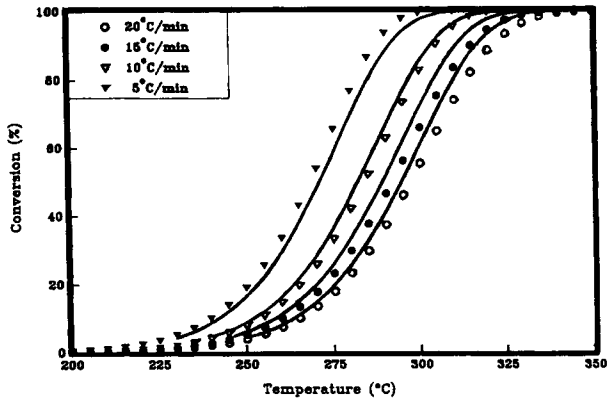

Figure 12 A comparison of the experimental and calculated degree of conversion of PMR-15 under DSC dynamic scans.

assumed to be the initiation of thermal polymerization of PMR-15. The comparison between the experimental and calculated results is shown in Figure 12. A good agreement existed between the experimental and calculated data. There was no sign of autoacceleration, which was often observed in free radical polymerizations with an initiator, but less pronounced in thermal polymerizations.[21] The reason was that, in a dynamic scan, the polymerizing chains were highly mobile at all temperatures, which implied that the mechanisms of reaction did not vary with changing temperatures. In poly-condensation reactions, the increase in molecular weight accompanied by a consequent increase in glass transition temperature often retarded the crosslinking reaction, which became diffusion controlled in the later stages of the reactions.[22] There was also no sign of retardation in the crosslinking reaction of PMR-15. A possible reason for this behavior was that, in addition polymerization, only very long chain polymers and monomers existed in the system. Monomers were highly mobile even in a gelled network, and the degree of reaction had little effect on the rate of reaction. The kinetic parameters calculated assuming a first-order curing reaction were also included in Table I.

Due to the incorporation of additional impurities and the dilution of reacting species, the monitoring of the curing reaction of the semi-IPN was more difficult. The curing kinetics of semi-IPNs of PMR-15 85%/LARC-TPI 15% and PMR-15 75%/LARC-TPI 25% were monitored by DSC. A scan rate of 10°C/min was employed. Because the PMR-15 resin was imidized and by the time when the crosslinking started, LARC-TPI had already been imidized, both polymers were quite stable. Therefore, no reaction between PMR-15 and LARC-TPI was assumed.

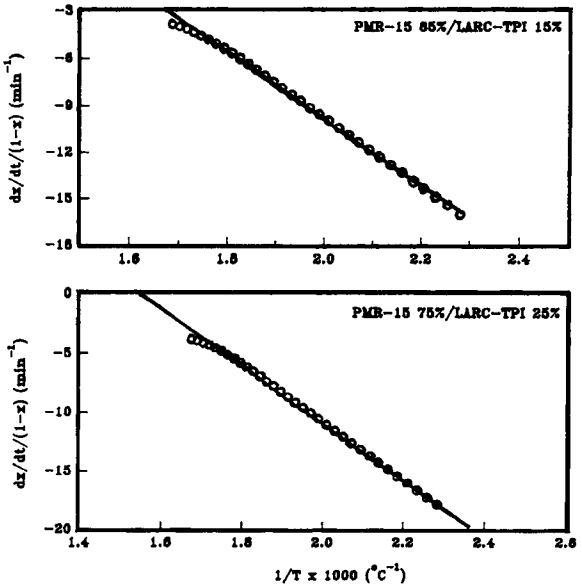

Figure 13 Linear regression on the dynamic DSC scan data of PMR-15/LARC-TPI semi-IPNs.

Thus, the observed reaction corresponded to the crosslinking of PMR-15.

The reaction order of the PMR-15 has already been shown to be 1. For simplicity, the curing of these semi-IPN systems was assumed to follow first-order kinetics. A plot of $\ln[dx/dt/(1-x)]$ vs. $1/T$ is shown in Figure 13. The following activation energies and preexponential factors were obtained by linear regression: E_a = 174 KJ/mol, A = 4.98 $\times 10^{15}$ min^{-1} for the PMR-15 85%/LARC-TPI 15% system and E_a = 199 KJ/mol, $A = 6.82 \times 10^{17}$ min^{-1} for the PMR-15 75%/LARC-TPI 25% system. These parameters are listed in Table I for comparison with their parent materials.

The degree of conversion of PMR-15/LARC-TPI semi-IPNs were measured by DSC at a rate of 10°C/

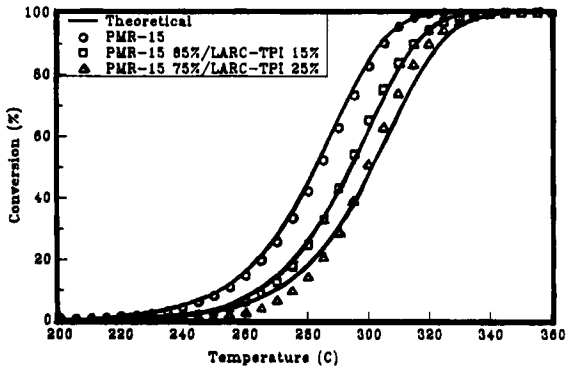

Figure 14 A comparison of the experimental and calculated degree of conversion of PMR-15 and its semi-IPNs.

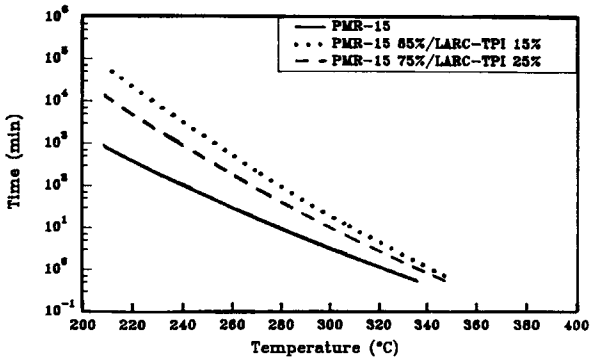

Figure 15 The predicted time needed for 95% completion of the cure of PMR-15 and its semi-IPNs.

min. The results are shown in Figure 14. The results of the study of PMR-15 are also included for comparison. As can be seen, it took longer time for semi-IPNs to complete the curing process at higher temperatures. The higher the weight fraction of LARC-TPI, the slower the crosslinking reaction proceeded. It is also interesting to note that the activation energies obtained for semi-IPNs were considerably larger than that of neat PMR-15, and E_a PMR-15 75%/LARC-TPI 25% > E_a PMR-15 85%/LARC-TPI 15% > E_a PMR-15. Again, the glass transition temperature played an important role here. PMR-15 prepolymer had a T_g of about 190°C, while imidized LARC-TPI had a T_g of about 250°C. The semi-IPN prepolymers had a higher T_g. The higher the weight fraction of LARC-TPI, the higher T_g the semi-IPN prepolymers had. Qualitatively, the reaction constant k can be written in the following form:

$$k = A \exp\left(-\frac{E_a}{RT}\right) = N_0 \exp\left(-\frac{E_d}{RT}\right) \exp\left(-\frac{E_a}{RT}\right) \quad (10)$$

where E_d is the diffusion controlled activation energy and is a function of glass transition temperature of the system, N_0 is a constant. A system with a higher T_g should have a higher E_d. The activation energies obtained contained two terms, one for the diffusion of the prepolymer, the other for the RDA reaction involved in the crosslinking reaction. A system of higher glass transition temperature had a higher activation energy due to the higher diffusion barrier for the reacting species.

The estimated times for 95% completion of the curing reaction for the PMR-15 and its semi-IPNs under isothermal condition are shown in Figure 15. These data provided a guideline for processing both PMR-15 and its semi-IPNs. In addition, these curves served to estimate the shelf life of PMR-15 and its semi-IPNs. From the results of Figure 15, it is concluded that the curing time needed for the semi-IPNs was considerably longer than that for neat PMR-15 at lower temperature due to the higher barrier of diffusion in the case of semi-IPNs. At higher temperatures, the barrier of diffusion could be neglected and the crosslinking reaction was controlled essentially by the RDA reaction. Under these conditions, the curing time needed for the three systems became very similar.

Although IR methods have been used for kinetics studies on these polymers,[23] they were utilized here mainly as complementary techniques. TGA or DSC techniques could give much more reliable and useful information in this regard.

A typical spectrum of PMR-15 is shown in Figure 16. The assignment of each peak was a formidable task. A possible assignment for each peak is listed in Table II.[23-26] The characteristic peaks for polyimide are 1780, 1722, 1372, 1179, 1089, and 717 cm^{-1} (see Table II). From the spectrum and the assignments, existence of impurities and significant peak overlaps were evident. For example, the anhydride peak of the asymmetric C=O stretching at 1780 cm^{-1} overlapped with that of the symmetric C=O stretching of imide ring. These impurities might come from the reacting monomers or from the side reaction in imidization and crosslinking. There were no apparent changes in the spectra obtained at different curing temperatures, especially for those characteristic of polyimides, which indicated that the extent of imidization was complete in the prepolymer.

A rigorous analysis of the spectra in the range of 800 to 900 cm^{-1} revealed some details of the crosslinking reaction, as shown in Figure 17. The spectra were obtained by staging PMR-15 at 110, 210, 285,

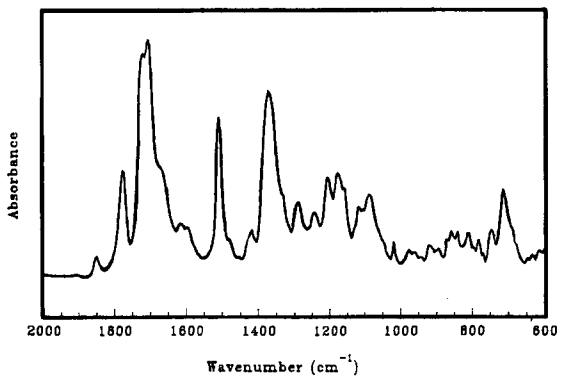

Figure 16 An FTIR spectrum of uncured PMR-15 at 210°C for 1 h.

and 355°C each for 1 h, respectively. The peak at 843 cm^{-1} was the characteristic band of the exo-exo geometric isomer of a norbornene end group, produced as an intermediate during the crosslinking reaction. As the curing temperature was raised from 210 to 285°C, this peak disappeared because of the crosslinking reaction. From Figure 15, to achieve 95% completion of cure, about 1000 min was required at 210°C, while only 10 min was needed at 285°C. When cured at an even higher temperature (355°C) for 1 h, the material exhibited a spectrum similar to that at 285°C. Hence, this peak was very useful for monitoring the crosslinking reaction. The existence of this peak even at a low curing temperature (110°C) also indicated that the as-received PMR-15 powder was slightly cured. It should be noted that the IR data was in good agreement with the kinetic results from DSC measurements.

The FTIR spectra of LARC-TPI staged at four different imidization temperatures are shown in Figure 18. The possible assignment for relevant peaks is listed in Table III.[18,23-26] The change in the spectra as imidization temperature changes was obvious: the imide peaks at 1781, 1722, 1367, and 713 cm^{-1} became very pronounced as the curing temperature was raised. From Figure 10, the times needed for 95% completion of imidization were several thousand minutes at 180°C, about 100 min at 220°C, and a few seconds at 285°C. The amide II peak at 1544 cm^{-1} characteristic of amic acid was

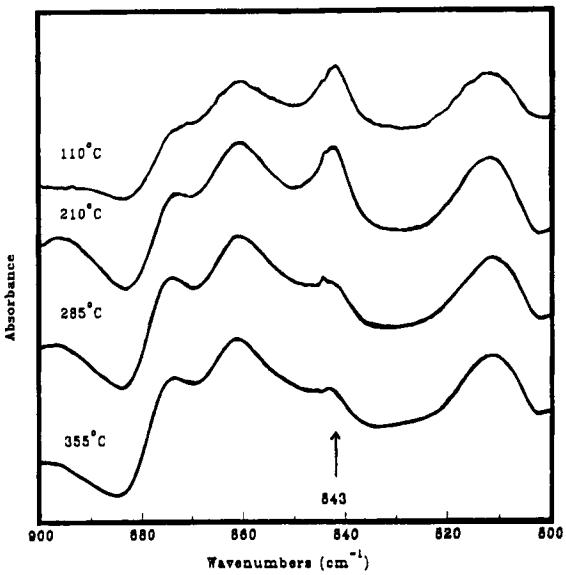

Figure 17 FTIR spectra around 843 cm^{-1} of PMR-15 at different temperatures for 1 h.

Table II IR Peak Assignments of PMR-15

Wavelength (cm^{-1})	Assignment
617	Characteristic of norbornene; Imide C=O bending.
717	Imide IV, C—N—C out plane vibration of imide ring or Olefinic C—H out of plane bending.
744	For Ph(COOH)(CO)—NH—Ph; Phenyl C—H out of plane bending.
785	C—H vibration of Norbornene exo-exo isomer.
811	Out of plane C—H deformation vibration of para-substituted aromatic ring.
842	Unique band of Norbornene endo-endo isomer.
862	Out of plane C—H deformation vibration of 1, 2, 4. substituted aromatic ring.
1021	Aryl C—H in-plane deformation of para substituted benzene, especially for Ph(COOH)(CO)NH—Ph and the like.
1089	Imide III, transverse stretching of cyclic imide $(OC)_2NC$.
1120	Imide III, transverse stretching of cyclic imide; Norbornene C—H_2 binding.
1179	C—N—C vibration of Imide ring.
1208	C—O—C stretching of cyclic anhydride.
1249	Amide III (NH bending + CN stretching), or carboxylic acid C=O absorption, along with 1290 peak.
1293	C=O stretching between 2 benzene ring, aromatic acid absorption or Imide III asymmetric C—N—C stretching.
1372	C—N—C symmetric stretching (axial vibration) of imide II.
1420	Amic acid.
1512	Aromatic ring C—H stretching, especially for NH—Ph—C—Ph—NH.
1680	C=O stretching of Ph(C—O)Ph or secondary amide (Amide I).
1708	Asymmetric C=O stretching of imide ring.
1722	Asymmetric C=O stretching of imide ring (Imide I) or C=O stretching of amic acid.
1780	Symmetric C=O stretching of imide ring (Imide I), Asymmetric C=O stretching of anhydride ring.
1854	Symmetric C=O stretching of anhydride ring.

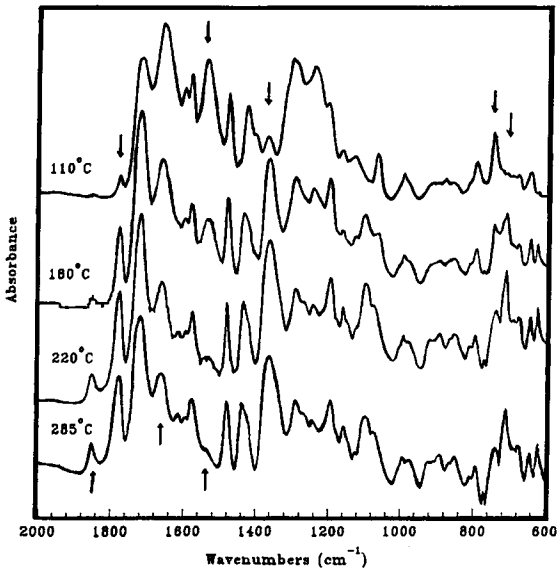

Figure 18 FTIR spectra of LARC-TPI at different temperatures for 1 h.

chosen to verify the DSC kinetic results. The peak was still very well-defined after imidization at 220°C for 1 h, but completely disappears as the curing temperature was raised to 285°C. The results shown in FTIR spectra were in good agreement with those observed in the DSC or TGA experiments.

It is also important to point out that at higher temperatures (above 180°C), the formation of anhydride was observed by the appearance of the 1854 cm^{-1} peak in the spectra. This was not uncommon in the imidization of poly(amic acid). As the temperature increased, the proportion of anhydride increased. Possible reasons were that the LARC-poly(amic acid) reverted in part to its BTDA monomer[27,28] or that chain scission of poly(amic acid) occurred with formation of anhydride.[29]

A suitable molding cycle for the new materials could be designed by making use of the kinetic results obtained. The approach developed here may also be used for curing cycle designs of other similar systems. The molding cycles are shown schematically in Figure 19. For LARC-TPI, the powder was first dried at 150°C for 30 min to remove absorbed moisture, then heated at 200°C for 30 min to eliminate most of the solvent and to partially imidize the resins. Next, the temperature was raised to 250°C to fully imidize the resins. By this time, the resins were almost volatile free and a pressure of 1.38 MPa was applied to compact the powders. Because LARC-TPI has a T_g at approximately 250°C,

Table III IR Peak Assignments of LARC-TPI

Wavelength (cm^{-1})	Assignment
626	Imide or amide O=C—N bending.
646	C—C—C vibration of aromatic ring.
713	Imide IV, C—N—C out plane vibration of imide ring.
742	For Ph(COOH)(CO)—NH—Ph or Phenyl C—H out of plane bending.
798	1,3-disubstituted aromatic ring.
855	Out of plane C—H deformation vibration of 1,2,4. substituted aromatic ring.
897	Aromatic skeletal vibration.
996	1,3-disubstituted aromatic ring.
1069	1,3-di or 1,2,4 tri-substituted benzene.
1100	Imide III, transverse stretching vibration of cyclic imide.
1162	Imide ring C—N—C transverse vibration, Imide III $(OC)_2NC$.
1200	C—O—C stretching of cyclic anhydride.
1247	Amide III (NH bending + CN stretching), or carboxylic acid C=O absorption, accompany with 1290 peak.
1295	C=O stretching between 2 benzene ring, or aromatic acid absorption.
1367	C—N—C axial vibration of imide ring.
1440	1,3 di- or 1,2,4-substituted benzene or Amide or COOH.
1484	C—C stretching of aromatic ring.
1544	Amide II (NH bending + CN stretching).
1582	1,2,4- or 1,3-substituted aromatic ring.
1606	Aromatic amide.
1664	C=O of Ph(C=O)Ph or secondary amide (Amide I).
1722	Asymmetric C=O stretching of imide ring or C=O stretching of amic acid.
1781	Symmetric C=O stretching of imide ring, Asymmetric C=O stretching of anhydride ring.
1855	Symmetric C=O stretching of anhydride ring.

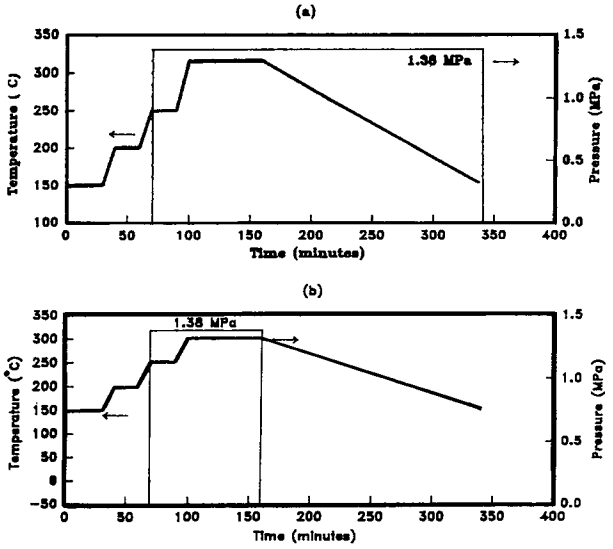

Figure 19 Molding cycle design for (a) LARC-TPI; (b) PMR-15 and their semi-IPNs.

the temperature was raised to 315°C to "melt" and shape the resin. The pressure was maintained during the slow cooling stage until the resins were fully solidified.

For PMR-15 and its semi-IPNs, the cure cycles were similar. A temperature of 200°C was used to imidize the amic acid and to eliminate any trapped volatile. The materials were still in their powder form because the PMR-15 prepolymer had a T_g of 190°C. At 250°C, as soon as the PMR-15 prepolymers began to "melt" and to lightly crosslink, a pressure 1.38 MPa was then applied. Finally, the temperature was raised to 300°C for 1 h to complete the crosslinking reaction. The pressure was dropped to mere contact pressure in the slow cooling stage, because the resin had already been cured and a high stress accompanied with mold shrinkage might cause cracks in the molded parts.

CONCLUSIONS

Proper processing of PMR-15 and its semi-IPNs is essential to optimizing the performance of these resins. Kinetic studies of PMR-15 and PMR-15/LARC-TPI semi-IPNs showed that the crosslinking reaction followed first-order kinetics. A reverse Diel–Alder reaction of the Norbornene end group in the cure of PMR-15 and its semi-IPNs was the controlling step. The glass transition temperature played an important role in the rate of cure. The semi-IPNs prepolymers, having higher T_gs, needed longer time to complete cure than the neat PMR-15 prepolymer. The semi-IPN of higher T_g had a higher activation energy due to the higher diffusion barrier for reacting species.

The imidization kinetics of LARC-poly(amic acid) could be followed satisfactorily by a two-step reaction scheme. The first step was the formation of a favorable conformation for cyclization involving residual solvent molecules, and this was a second-order reaction. The second step was the formation of imide rings, which involved the diffusion of water and solvent molecules. This step was diffusion controlled and the reaction behaved like a simple first-order reaction. This analysis supported the arguments that a decrease of molecular mobility due to an increase of glass transition temperatures accounted for the fast and slow cyclization phenomena.

Financial support for this project was provided in part by the NSF-EPSCoR program. B.Z.J. would like to thank Dr. Ruth Pater of NASA Langley for helping to provide a NASA-ASEE Summer Faculty Fellowship.

REFERENCES

1. J. N. Hay, J. D. Boyle, P. G. James, J. R. Walton, K. J. Bare, M. Konarski, and D. Wilson, *High Perform. Polym.*, **1**, 145 (1989).
2. Doug Wilson, *High Perform. Polym.*, **3**, 73 (1991).
3. D. Wilson, J. K. Wells, and J. N. Hay, *SAMPE J.*, **23**, May/June, 35 (1987).
4. R. D. Vannucci and K. J. Bowles, *SAMPE Q.*, **17**, January, 12 (1986).
5. A. C. Wong and W. M. Ritchey, *Macromolecules*, **14**, 825 (1981).
6. B. W. Kilhenny and J. L. Cercena, *Polyimides: Materials, Chemistry and Characterization*, C. Feger, M. M. Khojasteh, and J. E. McGrath, Eds., Elsevier, New York, 1989, p. 321.
7. G. D. Roberts and R. W. Lauver, *J. Appl. Polym. Sci.*, **33**, 2893 (1987).
8. R. W. Lauver, *J. Polym. Sci., Polym. Chem. Ed.*, **17**, 2529 (1979).
9. T. L. St. Clair, *Polymides*, D. Wilson, H. D. Stenzenberger, and P. M. Hergenrother, Eds., Blackie and Son Ltd., New York, 1990, p. 59.
10. D. J. Progar, T. L. St. Clair, and J. R. Pratt, *Polyimides: Materials, Chemistry and Characterization*, C. Feger, M. M. Khojasteh, and J. E. McGrath, Eds., Elsevier, New York, 1989, p. 151.
11. C. A. Pryde, *J. Polym. Sci., Polym. Chem. Ed.*, **27**, 711 (1989).
12. M. J. Brekner and C. Feger, *J. Polym. Sci., Polym. Chem. Ed.*, **25**, 2005 (1987).
13. R. H. Pater and C. D. Morgan, *SAMPE J.*, **24**, Sept/Oct, 25 (1988).
14. R. H. Pater and R. D. Partos, *Polyimides: Materials, Chemistry and Characterization*, C. Feger, M. M.

Khojasteh, and J. E. McGrath, Eds., Elsevier, New York, 1989, p. 37.
15. P. D. Frayer, *Polyimides, Synthesis, Characterization and Applications,* Vol. 1, K. L. Mittal, Ed., Plenum Press, New York 1984, p. 273.
16. F. W. Harris, *Polyimides,* D. Wilson, H. D. Stenzenberger, and P. M. Hergenrother, Eds., Blackie and Son Ltd., New York, 1990, p. 1.
17. L. A. Laius, Mi. I. Bessonov, Ye. V. Kallistova, N. A. Adrova, and F. S. Florinskii, *Polym. Sci. USSR,* **A9**(10), 2470 (1967).
18. H. J. Tai, Ph. D. Dissertation, Auburn University, 1992.
19. A. Hale and C. W. Macosko, *Macromolecules,* **24,** 2610 (1991).
20. K. C. Frisch, D. Klempner, S. Mifdal, H. L. Frisch, and H. Ghiradella, *Polym. Eng. Sci.,* **14,** 76 (1974).
21. W. H. Press, B. P. Flannery, S. A. Teukolsky, W. T. Vetterling, *Numerical Recipes,* Cambridge University Press, New York, 1986, p. 563.
22. Paul J. Flory, *Principles of Polymer Chemistry,* Cornell University Press, Ithaca, NY, 1953, p. 124.
23. K. Dusek and W. J. MacKnight, *Crosslinked Polymers, Chemistry, Properties and Applications,* ACS Symposium Series 367, Chapt. 1, R. A. Dickie, S. S. Labana, and R. S. Bauer, Eds., American Chemical Society, Washington, DC, 1988, p. 1.
24. S. F. Parker, N. D. Hoyle, and J. R. Walton, *High Perform. Polym.,* **2,** 275 (1990).
25. L. J. Bellamy, *The Infra-Red Spectra of Complex Molecules,* 3rd ed., Chapman and Hill, New York, 1975.
26. H. W. Siesler and K. Holland-Moritz, *Infra-Red and Ramam Spectroscopy of Polymers,* Marcel Dekker, New York, 1980, p. 52.
27. I. K. Varma, R. N. Goel, and P. S. Varma, *J. Polym. Sci., Polym. Chem. Ed.,* **17,** 703 (1973).
28. K. N. Ninan, K. Krishnan, and J. Mathew, *J. Appl. Polym. Sci.,* **32,** 6033 (1986).
29. M. I. Tsapovetsky and L. A. Laius, *Polyimides: Materials, Chemistry and Characterization,* C. Feger, M. M. Khojasteh, and J. E. McGrath, Eds., Elsevier, NewYork, 1989, p. 379.

Received July 13 1994
Accepted July 2 1995